Neuroscience Letters 736 (2020) 135294

Contents lists available at ScienceDirect

Neuroscience Letters

journal homepage: www.elsevier.com/locate/neulet

Research article

GABA, noise and gain in human visual cortex

Stephen T. Hammett, Emily Cook, Omar Hassan, Ceri-Ann Hughes, Hanna Rooslien, Rana Tizkar, Jonas Larsson*

Department of Psychology, Royal Holloway University of London, Egham TW20 0EX UK

ARTICLE INFO

Keywords:
GABA
visual cortex
neural noise
gain
inhibition
suppression
contrast discrimination

ABSTRACT

High levels of GABA (gamma-aminobutyric acid, the brain's primary inhibitory neurotransmitter) are associated with enhanced cognitive and perceptual performance. It has been proposed that these effects result from GABA reducing neural noise or variability, but the precise mechanisms remain unknown. We have measured how individual differences in GABA concentration in the visual cortex are related to performance on a visual contrast discrimination task. Our results reveal that the facilitatory strength of the typical "dipper" function elicited by this task is strongly correlated with GABA concentration. A simple, biologically plausible, network model comprising excitatory and suppressive neural populations accounts for the data well and indicates that the strength of suppression increases as GABA concentration increases. Inter-individual variations in GABA were correlated both with the inhibition strength of the model (mimicking the effect of GABA) and, inversely, with the magnitude of the response criterion. This enhanced suppression has the dual effect of suppressing noise and reducing the gain of the neural response. Our findings thus suggest that the changes in performance conferred by high GABA concentration are mediated by both a reduction of noise and, paradoxically, a reduction in neural, but not perceptual, sensitivity.

1. Introduction

High concentrations of GABA are known to enhance human perceptual and cognitive performance [1,2,3,4,5]. This relationship is likely to be causal rather than correlational, as evidenced by the finding that the GABA agonist Lorazepam increases suppression duration in bistable figure perception [6]. It has been suggested that GABA enhances performance by reducing variability or noise. For instance, Sumner et al [2] suggested that the reduction in the effect of distractors on a motor task found in those with high levels of GABA might be due its ability to effectively suppress the distractors. Similarly, Sandberg et al [4] suggest that GABA may enhance cognitive function by either suppressing irrelevant signals or enhancing relevant neural representations. However, the precise mechanisms by which GABA exerts these effects remain unknown. To explore this question, we have investigated how the "dipper effect" observed in measurements of visual contrast discrimination thresholds, and which has been suggested to reflect the level of intrinsic neural noise, depends on GABA levels in the visual cortex. We used a simple visual task in which subjects identified which of two grating stimuli (Fig. 1A) had the higher contrast for a range of different base or "pedestal" contrasts. The resulting plots of contrast detection thresholds against pedestal contrast show a characteristic dip (enhanced sensitivity) at low, but non-zero, pedestal contrasts (Fig. 1B, C). It is typically assumed that this improvement in sensitivity is due to either the shape of the contrast-response function (CRF) describing the neural population response to a stimulus, the suppression of noise driven by the non-zero pedestal stimuli (akin to uncertainty reduction), or both [7]. Based on GABA's proposed role in suppressing noise, we predicted that individual variations in GABA levels would be associated with variations in the magnitude of the dipper effect, a prediction that was borne out by our results. To characterise how modulations of cortical responses by GABA can account mechanistically for this effect, we fit a biologically plausible network model of neural population activity to our data. The results of this model fit suggest that GABA not only reduces noise, but also changes the gain of neural responses, a finding that has wider implications for understanding the role of GABA in modulating behaviour.

2. Methods

2.1. Subjects

An opportunity sample of fifteen subjects participated in the experiment. All had normal or corrected-to-normal vision. One subject's

* Corresponding author.
E-mail address: jonas.larsson@rhul.ac.uk (J. Larsson).

https://doi.org/10.1016/j.neulet.2020.135294
Received 10 January 2020; Received in revised form 3 August 2020; Accepted 3 August 2020
Available online 07 August 2020

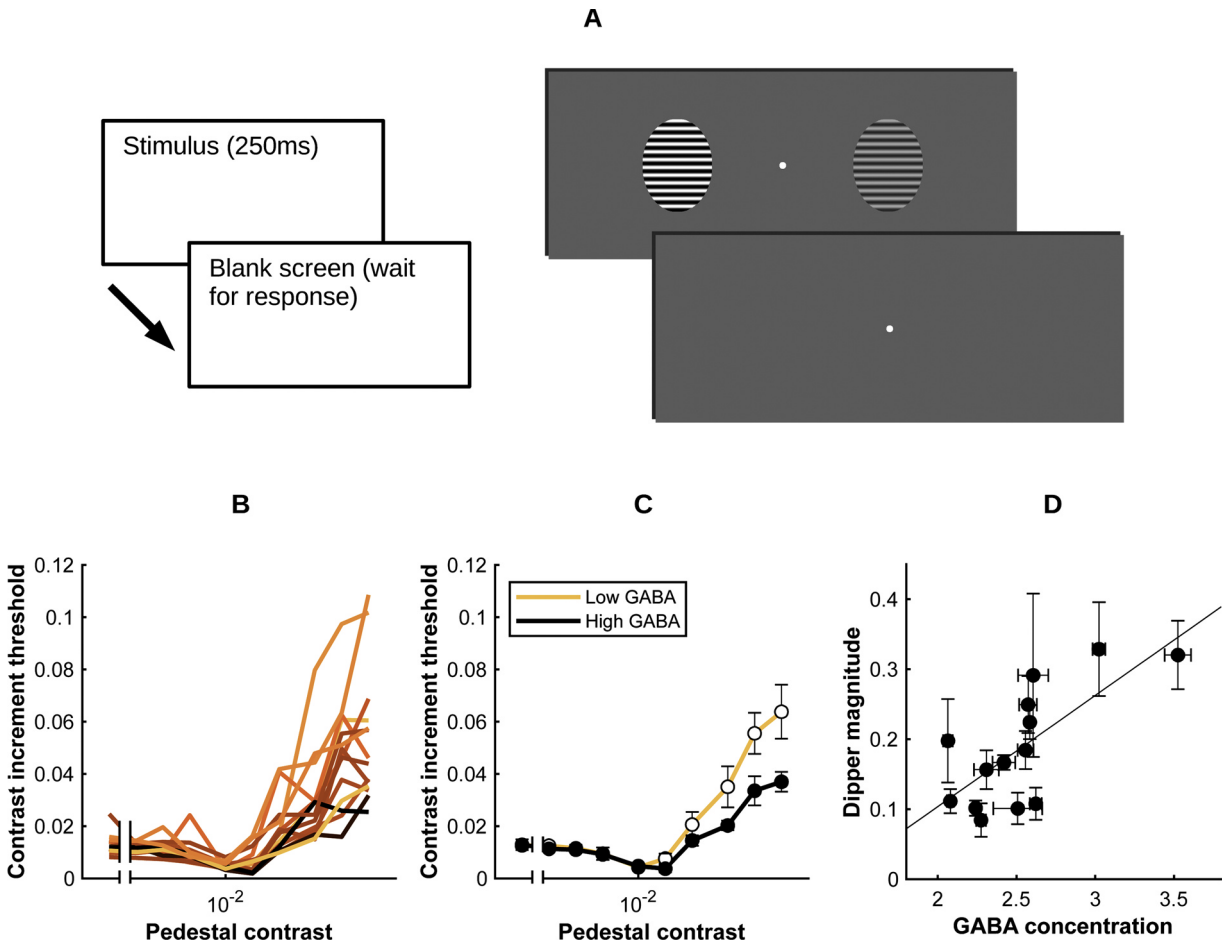

Fig. 1. A. Experimental design. Stimuli consisted of two grating patches shown either side of a fixation spot for 250 ms; subjects indicated which patch had higher contrast.. . B. Measured dipper functions for all subjects. Colour indicates GABA concentration (lighter – low, darker – high). C. Average dipper function for low GABA (GABA < mean) and high GABA (GABA > mean) subjects. Each line represents the average of 7 subjects dipper functions. Error bars, standard error of the mean. D. Cortical GABA concentration correlates with DM ($r = 0.71$, $P = 0.0041$). Y error bars, bootstrapped 68% confidence intervals (~ 1 standard deviation); X error bars, range of GABA measurements.

data was discarded as the measured contrast thresholds at the five lowest pedestal contrasts were highly variable between blocks (individual threshold error [SD of threshold estimates] > 2 SDs above the mean error across subjects). The results below are from the 14 remaining subjects.

2.2. Contrast discrimination measurement

All stimuli were horizontally oriented sinusoidal gratings of 6 c deg^{-1} displayed on an Eizo 6600-M monochrome CRT whose mean luminance was 20 cd m^{-2}. The display subtended 34 degrees horizontally by 24 degrees vertically. Stimuli were presented in hard-edged elliptical windows that subtended 1.5° horizontally and 2° vertically and were situated equidistant of a small white fixation point, presented continuously in the centre of the screen. The windows were separated horizontally by 3 degrees (eccentricity of the centre of each window was 2.25°). Viewing distance was 57 cm. Subjects viewed the screen binocularly using a head and chin rest.

Contrast increment detection thresholds were estimated using a 2-alternative forced choice procedure. On each trial, subjects were shown two stimulus patches on either side of a fixation marker and indicated by a button press which patch had the higher contrast (Fig. 1A). Trials began by displaying the fixation marker for 5 seconds, after which the stimulus patches were shown for 250 ms, after which only the fixation marker was shown until the subject responded by pressing a button. Once the response button had been pressed the screen remained blank for 1 s before the onset of the next trial. Trials were run back-to-back in blocks of 50 trials.

Gratings were shown at one of 10 pedestal contrasts (0 to 0.4) in separate blocks. On each trial one of the gratings (randomly left or right) was shown at slightly higher contrast, with contrast increments adjusted by an adaptive staircase procedure [8] to obtain a threshold estimate corresponding to 82% correct. For each pedestal contrast four blocks were run and threshold estimates averaged across blocks. We quantified the dipper magnitude (, DM) as the difference between the zero pedestal contrast threshold (absolute threshold) C_0 and the minimum increment threshold C_{min}, divided by the maximum threshold C_{max}:

$$DM = \frac{C_0 - C_{min}}{C_{max}} \quad (1)$$

2.3. Modelling

Dipper functions were fit with a model derived from Boynton et al [9]. In this model, the dipper function arises from an accelerating non-linearity in the CRF at low pedestal contrasts. The model assumes that contrast detection thresholds correspond to a fixed internal response difference (criterion) Δr between the pedestal contrast c and the target contrast $c+\Delta c$. Under this assumption, the contrast increment required for threshold detection Δc corresponds directly to the slope of the CRF at each pedestal contrast, such that steeper slopes result in smaller

increment thresholds. We used a sigmoid CRF that has previously successfully fit psychophysical, electrophysiological and fMRI data [9,10,11,12,13] given by

$$R(C) = a\frac{c^{p+q}}{c^q + \sigma^q} \quad (2)$$

where *R(C)* is the response at contrast *C*, *a* is an arbitrary scale factor that determines the maximum response, *p* and *q* exponents govern the shape of the sigmoid, and σ determines the contrast at which the function changes shape. From this function, for a fixed response criterion difference Δr, the contrast increment threshold Δc at pedestal contrast *c* can be approximated by the difference in contrasts between *c* and the contrast corresponding to the response to the pedestal contrast, plus the response difference criterion Δr:

$$\Delta c = C(R(c) + \Delta r) - c = R^{-1}(R(c) + \Delta r) - c \quad (3)$$

where $C(R) = R^{-1}$ denotes the "response-contrast function", i.e., the inverse of the contrast response function. The inverse was computed numerically from the CRF (2) by creating a look-up table for 10,000 contrasts between 0 and 1 (maximum contrast).

Nelder-Mead simplex minimisation was used to fit equation (3) to measured dipper functions, holding *a* fixed at 1 while allowing the remaining parameters to vary freely. To avoid larger, more variable threshold values from biasing the fit and ensure that the fitted curve accurately captured the dip at the lowest contrasts, each data point was weighted by a value proportional to the inverse of the measurement error. As an estimate of the error we used the mean of the threshold estimate for each contrast, rather than the standard deviation, as the small number of measurements (4 per pedestal contrast) meant that standard deviation estimates were much less robust and variable than the mean. This was conceptually equivalent to weighting by the standard deviation, as this measure scaled with the mean threshold ($r = 0.82$, $P < 0.0001$; Supplementary Fig. 1). As a comparison we also ran the fits without weights, but the resulting fitted curves failed to fully capture the dip at lower contrasts. Initial values of *p* and *q* were set to 0.3 and 2 respectively as in Boynton et al. [9] The initial value of Δr was set to 0.1 (i.e., 10% of the maximum response) and σ set to the contrast corresponding to the minimum contrast increment threshold. We fit the model with a range of initial values for these four parameters to ensure that the resulting fit was not strongly dependent on starting parameters.

In a follow-on analysis we modified the CRF to include a quasi-mechanistic model of neural inhibition by replacing equation (2) with the Wilson-Cowan recurrent network model [14], comprising one excitatory and one inhibitory population which have recurrent connections both with themselves and with one another. The strength of these connections is given by the four parameters J_{ei} and J_{ie} (inter-population) J_{ee} and J_{ii} respectively (intra-population). The activity of this network is described by two coupled differential equations:

$$\tau\, dE / dt = E + g_e[J_{ee}E - J_{ei}I + e(t)] \quad (4)$$

$$\tau'\, dI / dt = I + g_i[J_{ie}E - J_{ii}I + i(t)] \quad (5)$$

where τ and τ' are the time steps or constants corresponding to membrane time constants for the excitatory and inhibitory populations, and *e(t)* and *i(t)* the external input to the excitatory and inhibitory populations, respectively. $g_e(x)$ and $g_i(x)$ are the response functions, representing the proportion of cells firing for any given input value, for the excitatory and inhibitory populations. We used *R(C)* given in (2) as the response function for both $g_e(x)$ and $g_i(x)$, with initial parameters derived by fitting equation (2) to the mean dipper function ($\Delta r = 0.048$, $\sigma = 0.011$, $p = 0.59$, $q = 3.79$). For equations (4) and (5) the following initial parameters were used: $\tau = 10$ ms, $\tau' = 20$ ms, $e(t) = i(t) = c$ (input contrast), initial activities $E = I = 0$, $J_{ei} = 0.25$, $J_{ie} = 0.5$, $J_{ee} = 0.4$, $J_{ii} = 0.25$. Parameter values were chosen based on previous research using this model [15]. The results were qualitatively similar for different values for the fixed parameters provided all weights were of similar magnitude. The ode45 solver in Matlab was used to determine the steady-state output (defined as the excitatory response, *E*, at 500 ms post-stimulus) of each of the two populations for each input contrast. The resulting output response plotted against contrast yielded a contrast-response function *R(C)* incorporating the effects of recurrent excitation and inhibition. This function was substituted into equation (3) and used to fit to the measured dipper functions in the same way as for the original model, allowing J_{ei} and/or Δr to vary while keeping all other parameters constant.

2.4. GABA measurement

Visual cortical GABA concentration was estimated using magnetic resonance spectroscopy (MRS) [16]. MRS data were acquired on a 3 T whole-body MR scanner (Magnetrom Trio: Siemens, Erlagen, Germany) using the MEGAPRESS sequence (TR 2000 ms, TE 68 ms). The MRS voxel (30 × 35 × 25 mm) was placed over the calcarine cortex. To guide voxel placement, T2-weighted localiser images covering the visual cortex in the three cardinal planes (in-plane resolution 0.4 × 0.4 mm, slice thickness 3 mm) were acquired prior to MRS acquisition; these images were also used for tissue segmentation (Supplementary Fig. 2). Each subject underwent 2 GABA scans (using an editing pulse to isolate the GABA signal) and 2 reference scans (no editing pulse and unsuppressed water signal) in alternating order, starting with GABA acquisition. GABA concentration was estimated from pairs of GABA and reference scan data using the Gannet toolbox [16] (Supplementary Fig. 3). Four estimates of GABA were computed from the full set of combinations of GABA and reference scans, and the result averaged.

2.5. Correction for voxel tissue composition

We estimated the proportion of GM, CSF, and white matter (WM) within the MRS voxel in each subject by segmenting the T2-weighted localiser images into 3 tissue classes using the FSL "fast" program [17]. The proportion of each tissue label within the volume covered by the MRS voxel was estimated for each of the three images by creating a mask image of the MRS voxel (resampled to the localiser image format) and counting the number of voxels located within the MRS voxel mask that belonged to each tissue class. The results for the three images were averaged. Due to poor GM/WM contrast in the localiser images, estimates of GM and WM proportions were quite variable within subjects, whereas CSF estimates showed a high degree of consistency. Hence, we used the CSF proportion ($Prop_{CSF}$) to compute a tissue correction factor for the GABA estimates as follows, which corrects for the fact that CSF contains virtually no GABA:

$$GABA_{adj} = GABA_{raw} / (1\text{-}Prop_{CSF}) \quad (6)$$

In the results GABA refers to the adjusted GABA estimates throughout.

3. Results

All subjects displayed a clear dipper effect : as pedestal contrast increased from zero, contrast increment thresholds initially decreased with a minimum around 1% contrast (Fig. 1B). DM was strongly correlated with cortical GABA concentration, with higher GABA concentrations associated with larger DM ($r = 0.71$, $P = 0.0041$) (Fig. 1D). GABA concentrations were not significantly correlated with either zero pedestal contrast threshold ($r = -0.026$, $P = 0.93$) or the minimum contrast increment threshold ($r = -0.37$, $P = 0.19$). There was a non-significant trend for a negative association between GABA and the contrast increment threshold at maximum pedestal contrast ($r = -0.52$, $P = 0.059$). Subjects with high levels of GABA had systematically lower

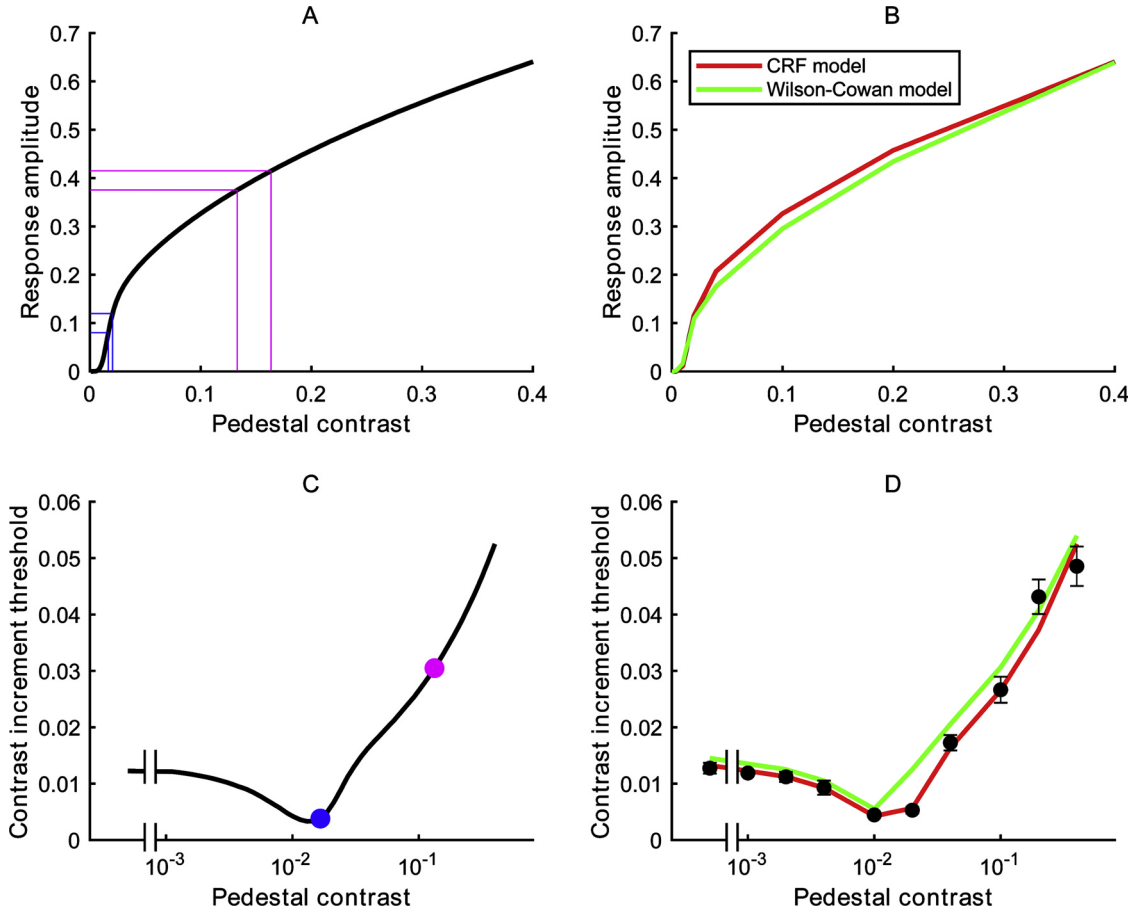

Fig. 2. A. A non-linear CRF predicts the dipper effect if subjects require a fixed response increment to detect a contrast increment. The contrast increment will be smaller when the slope of the CRF is large (blue lines) than when the slope is small (purple lines). B. CRFs fit to the mean dipper function (averaged across subjects). The CRF model (red) and the Wilson-Cowan model (green) yield similar CRFs. C. Predicted dipper function using the CRF in A. Blue and purple dots correspond to the contrast interval between the blue and the purple lines respectively shown in panel A. D. Mean dipper function fit with the two models. Black symbols, measured contrast increment thresholds at each pedestal contrast, averaged across subjects. Both the CRF model (red) and the Wilson-Cowan model (green) account for the dip in contrast increment thresholds at low pedestal contrasts relative to zero pedestal contrast.

contrast increment thresholds at higher pedestal contrasts (Fig. 1C). To test whether this difference was significant, we split the subjects into low (GABA < mean GABA) and high (GABA > mean GABA) groups and compared the groups using a 2-way mixed ANOVA with pedestal contrast and low/high GABA as factors. The interaction between pedestal contrast and low/high GABA was significant [$F(9,108) = 4.86$, $P < 0.0001$]. DMs also differed significantly between the low and high GABA groups (Kolmogorov-Smirnov 2-tailed test, $P = 0.028$).

3.1. Modelling

We explored whether a standard CRF, with the assumption of a contrast-invariant criterion shift in response (equations 2 and 3; hereafter, the "CRF model"), could predict the observed dipper functions and account for inter-individual variability in the size of the dipper. This model was fit to the mean dipper function (averaged across subjects). The model accurately replicated the shape of the measured function (Fig. 2D, red line). Simulations showed that all of the model parameters Δr, σ, p or q influenced the magnitude of simulated dippers, but each one had distinct effects on the shape of the dipper (Supplementary Fig. 4). To determine which parameter could best account for inter-individual differences in DM, we fit the dipper functions for each subject separately, allowing each one of Δr, σ, p or q to vary while keeping all other parameters fixed at the values obtained by fitting the mean dipper function (Supplementary Figs. 5–8). Whilst Δr and σ were found to correlate with DM in opposite directions ($r = -0.63$, $P = 0.031$ and $r = 0.88$, $P = 0.0004$ respectively; Supplementary Fig. 9), neither p nor q correlated with DM ($r = 0.41$, $P = 0.21$ and $r = -0.17$, $P = 0.57$ respectively) (all model fit P-values False Discovery Rate corrected for multiple comparisons).

Given the association between DM and GABA concentration, we investigated if these parameters might also correlate with variations in GABA concentrations across subjects. Δr and σ showed evidence of an association with GABA, although the association only reached statistical significance for σ (Δr: $r = -0.52$, $P = 0.12$; σ: $r = 0.66$, $P = 0.043$; Supplementary Fig. 9). Neither p nor q were significantly correlated with GABA ($P > 0.4$ and $P > 0.5$ respectively).

These results suggest two distinct mechanisms by which GABA could modulate contrast thresholds. Firstly, for a fixed-performance task such as the one used in this study, a reduction in the response criterion Δr implies a corresponding reduction in the width of the noise distributions, suggesting that GABA could modulate the criterion by reducing neural noise. Secondly, an increase in the σ parameter leads to a rightward shift of the underlying neural CRF, suggesting that higher concentrations of GABA result in a reduction in neural contrast gain. Importantly however, neither parameter on its own accounts fully for the interindividual differences in dipper functions. A reduction in Δr results in an overall reduction of contrast thresholds, particularly at the highest pedestal contrasts (Supplementary Fig. 4). If GABA levels determine neural noise and thus response criterion, high GABA concentrations should be associated with reduced thresholds at high and low pedestal contrasts. However, we found no correlation between

GABA and zero pedestal contrast thresholds. Conversely, an increase in σ shifts the CRF rightwards along the contrast axis and thus increases the contrast increment required to generate a response increment equal to the response criterion at low pedestal contrasts (Supplementary Fig. 4, Fig. 2A), but only marginally changes increment thresholds at high pedestal contrasts (Supplementary Fig. 4). Given the positive correlation between σ and GABA, we would therefore have expected high GABA concentrations to be associated with an increase in thresholds at zero pedestal contrast, a pattern that was not present in our data. A possible explanation is that GABA modulates both Δr and σ but in opposite directions (i.e., reducing Δr and increasing σ), resulting in a net null effect on zero pedestal contrast thresholds while accounting for the individual variability in DM (and the trend for reduced contrast thresholds at high pedestal contrasts with high GABA).

Whilst this interpretation provides a description of the effect of GABA on neural responses, it does not explain how these changes come about. Given that GABA mediates neural inhibition, we explored whether a more realistic network model of neural responses that incorporated neural excitation and inhibition, analogous to that found in real visual cortical circuits, could account for these changes. We used Wilson & Cowan's recurrent network model [14] which describes the activity of two coupled populations of neurons, one excitatory and one inhibitory that receive a common input (Fig. 3A). In this model, the weight parameter which most closely approximates the effect of GABA is J_{ei}, which quantifies the input to the excitatory population from the inhibitory one (i.e., the strength of inhibition). The effect of changing the value of this parameter was similar to changing σ in the original model – shifting the CRF horizontally (Supplementary Fig. 10). To test whether changes in this weight – analogous to changes in GABA – could account for the variation in dipper functions and DM across subjects, we fit the model to individual dipper functions, allowing J_{ei} to vary while keeping other parameters constant. While this model did not provide as close fits as the original model (Supplementary Fig. 11), the fitted J_{ei} parameter was strongly correlated with both DM ($r = 0.76$, $P = 0.0034$) and GABA ($r = 0.65$, $P = 0.012$) across subjects (Fig. 3B). This parameter also accounted for the observation that subjects with high GABA had the minimum of the dipper function (the minimum increment contrast threshold) shifted to a higher pedestal contrast than the low-GABA subjects (Figs. 1C, 3 C–D). Analogous to the effect of σ in the original model, the rightward shift of the underlying CRF associated with larger values of J_{ei} (i.e., stronger inhibition) predict an increase in thresholds at zero pedestal contrast, which were not observed in the measured dippers (Fig. 3C). We therefore evaluated the effect of simultaneously fitting the criterion parameter Δr (Fig. 3D). This resulted in an improved overall fit of individual functions (Supplementary Fig. 12) while the correlation between J_{ei} and GABA ($r = 0.69$, $P = 0.03$) and J_{ei} and DM ($r = 0.60$, $P = 0.032$) remained, and also predicting the rightward shift in the location of the dipper minimum associated with high GABA (Fig. 3D). The criterion parameter Δr was significantly correlated with DM ($r = -0.63$, $P = 0.03$), though not with GABA ($r = -0.46$, $P = 0.095$). These results suggest that GABA modulates DM by reducing the gain of the CRF whilst simultaneously reducing neural noise, resulting in no overall effect of GABA on absolute contrast thresholds.

4. Discussion

Previous studies [5,18] have demonstrated a strong association between GABA and behavioural measures of visual inhibition. Our results are consistent with these findings and indicate that contrast discrimination thresholds for low pedestal contrasts decrease above absolute threshold. This facilitation is strongly associated with GABA. There are two categories of models that can account for this facilitatory effect. The first type of model, a variant of which was used in the present study, explains the effect as a result of changes in the slope of a non-linear contrast-response function that describes the neural population response [19] (Fig. 2). Alternatively, facilitation can be modelled as the result of an effective reduction in noise at low pedestal contrasts [20]. For instance, if we assume that discrimination is based upon detection of the highest response to two stimuli, at threshold this highest response may well be derived from a spurious noisy response from a neural population unrelated to the stimulus rather than a neural population sensitive to the stimulus itself. Above threshold, the responses will be dominated by neural populations sensitive to the stimulus and thus the effect of noise is reduced. A variant of this model ascribes the noise reduction to stimulus-evoked inhibition by the pedestal stimulus, which is greater at low than zero pedestal contrasts. Our results reconcile these two types of model by demonstrating that both are in fact necessary to account for GABA-associated inter-subject variations in DM and contrast sensitivity. We find that these variations are best explained by increasing GABAergic inhibition causing a rightward shift of a non-linear CRF in a recurrent network model (akin to a reduction in response gain), in combination with a reduction in the response criterion (akin to a reduction in noise). Specifically, we find that a model that incorporates changes only in either gain or noise cannot account for the measured dipper functions. This result is both biologically plausible and consistent with physiological data. GABA's effects in cortical circuits is primarily mediated by a combination of hyperpolarisation and shunting inhibition. Such inhibition would be predicted to reduce the likelihood of spurious or spontaneous spikes (suppressing noise) and increase the stimulus strength required to induce a spike (reducing gain). Although this reduction in gain reduces sensitivity of a single neuron, this is counteracted by the reduction in noise in the population of neurons, such that at the level of the observer contrast sensitivity is enhanced at higher pedestal contrasts when inhibition is strong (Fig. 4D). Our model thus makes the somewhat paradoxical prediction that the enhanced contrast sensitivity in individuals with high levels of GABA is associated with a *decrease* in sensitivity at the neuronal level.

Our results have implications that go beyond the question of the origin of the dipper function. A growing body of evidence indicates that high concentrations of GABA is associated with enhanced performance over a range of perceptual and cognitive tasks [1–5], and it has been proposed that these effects are due to GABA suppressing noise [1,2,5]. Our results indicate that the effects of GABA on these higher level functions is likely to involve not just noise suppression but also changes in neuronal gain. This observation suggests potential new strategies to probe the effects of GABA on cognitive performance. For instance, it has been shown that attention can modulate the gain of motion-sensitive neurons in area MT [21]. We predict that individual variations in GABA should likewise affect the gain of these neurons, which could be probed by measuring individual variations in motion sensitivity. Given that GABA levels correlate with surround suppression [5], such an approach might also be a way to probe interactions between attention and suppression proposed by some models of attention [22].

A number of studies have pointed toward GABA's role in noise or distractor suppression but, to date, the mechanisms by which these suppressive effects may be realised has not been documented. Our results indicate that a recurrent network model incorporating excitatory and inhibitory populations offers a viable candidate for how GABA mediates suppression at the system level. The model fits are consistent with a scheme whereby GABA reduces neural response gain but simultaneously reduces noise. Thus, the facilitatory effect of GABA appears to be mediated by suppressing excitatory neural responses in a manner that simultaneously changes the gain of the neural response and reduces the effective noise in the system.

CRediT authorship contribution statement

Stephen T. Hammett: Conceptualization, Methodology, Formal analysis, Software, Supervision, Writing - original draft, Writing - review & editing. **Emily Cook:** Investigation. **Omar Hassan:**

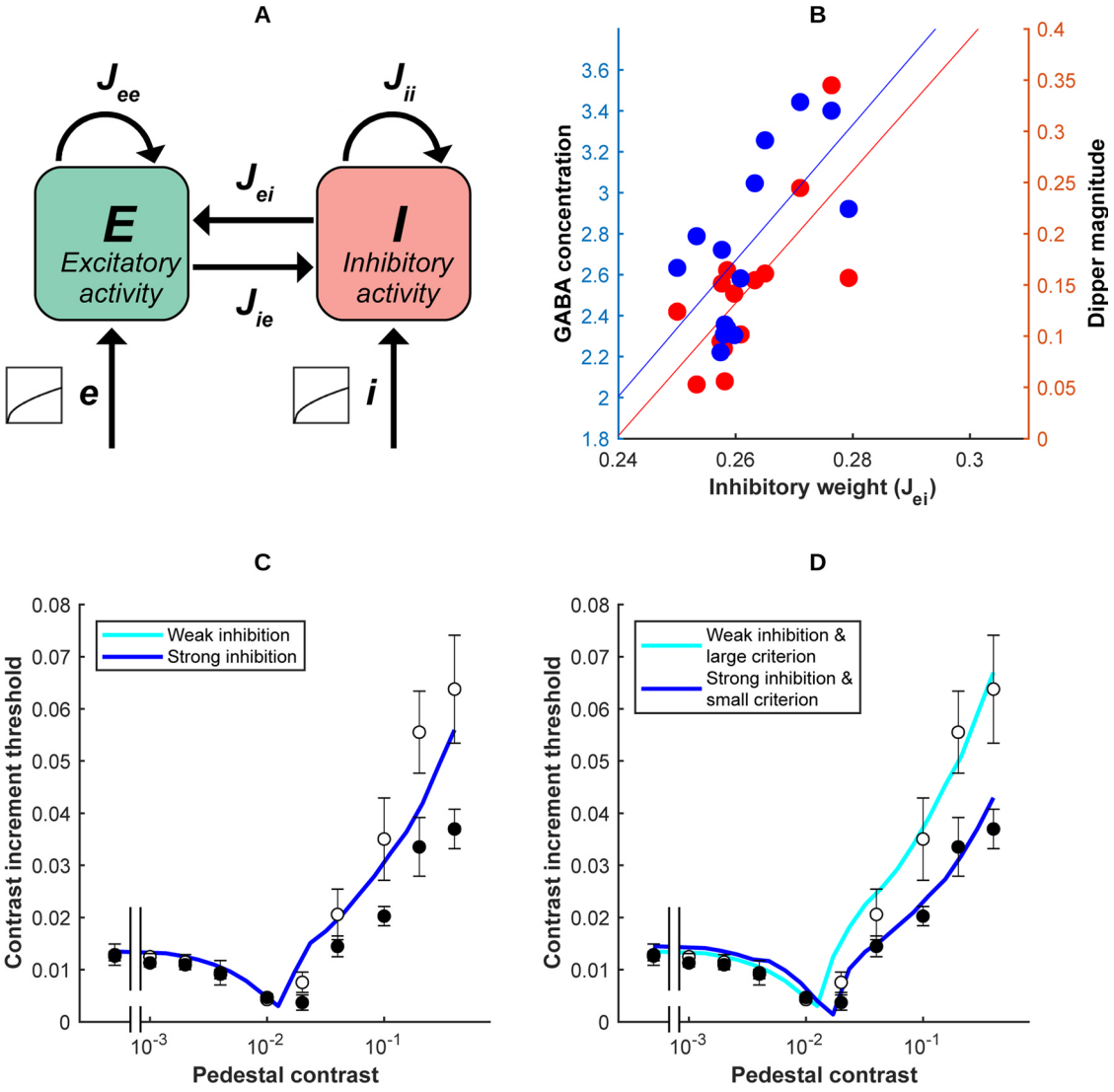

Fig. 3. A. The Wilson & Cowan model. E and I represent the pooled activity of the excitatory and inhibitory neural populations respectively, e and i are the external input to the respective populations (here, $e = i$) and J_{xx} are weights describing the strength of inter- and intrapopulation connections. B. The strength of inhibition J_{ei} predicts inter-individual variations in GABA concentration (blue symbols) and DM (red symbols). Values along the x axis correspond to the inhibitory weights J_{ei} from fitting a Wilson-Cowan model to the dipper function of each subject. C. The strength of inhibition J_{ei} accounts for the rightward shift of dipper function minimums in high-GABA individuals (filled circles) relative to low-GABA individuals (open circles), but incorrectly predicts an increase in thresholds at low contrasts for high-GABA subjects. D. Incorporating a reduction in response criterion Δr with higher levels of GABA accounts both for the rightward shift in dipper minimum and the reduction in thresholds at high pedestal contrasts.

Investigation, Software. **Ceri-Ann Hughes:** Investigation. **Hanna Rooslien:** Investigation. **Rana Tizkar:** Investigation. **Jonas Larsson:** Conceptualization, Methodology, Formal analysis, Software, Supervision, Visualization, Funding acquisition, Writing - original draft, Writing - review & editing.

Appendix A. Supplementary data

Supplementary material related to this article can be found, in the online version, at doi:https://doi.org/10.1016/j.neulet.2020.135294.

References

[1] R. Edden, S. Muthukumaraswamy, T. Freeman, K. Singh, Orientation discrimination performance is predicted by GABA concentration and gamma oscillation frequency in human primary visual cortex, J. Neurosci. 29 (2009) 15721–15726.
[2] P. Sumner, R. a E. Edden, A. Bompas, C.J. Evans, K.D. Singh, More GABA, less distraction: a neurochemical predictor of motor decision speed, Nat. Neurosci. 13 (2010) 825–827.
[3] E.C. Porges, et al., Frontal Gamma-Aminobutyric Acid Concentrations Are Associated With Cognitive Performance in Older Adults, Biol. Psychiatry Cogn. Neurosci. Neuroimaging 2 (2017) 38–44.
[4] K. Sandberg, et al., Occipital GABA correlates with cognitive failures in daily life, Neuroimage 87 (2014) 55–60.
[5] E. Cook, S.T. Hammett, J. Larsson, GABA predicts visual intelligence, Neurosci. Lett. 632 (2016) 50–54.
[6] A.M. Van Loon, et al., GABA shapes the dynamics of bistable perception, Curr. Biol. 23 (2013) 823–827.
[7] J. Solomon, The history of dipper functions, Atten. Percept. Psychophys. 71 (2009) 435–443.
[8] A.B. Watson, QUEST: A general multidimensional bayesian adaptive psychometric method, J. Vis. 17 (2017) 1–27.
[9] G.M. Boynton, J.B. Demb, G.H. Glover, D.J. Heeger, Neuronal basis of contrast discrimination, Vision Res. 39 (1999) 257–269.
[10] A.B. Bonds, Role of inhibition in the specification of orientation selectivity of cells in the cat striate cortex, Vis. Neurosci. 2 (1989) 41–55.
[11] D.G. Albrecht, W.S. Geisler, Motion Selectivity And The Contrast-Response Function Of Simple Cells In The Visual Cortex, Vis. Neurosci. 7 (1991) 531–546.
[12] J.M. Foley, Human luminance pattern-vision mechanisms: masking experiments require a new model, J. Opt. Soc. Am. A 11 (1994) 1710.
[13] J.M. Foley, G.M. Boynton, A new model of human luminance pattern vision mechanisms: Analysis of the effects of pattern orientation, spatial phase and temporal frequency, Computational Vision Based on Neurobiology SPIE 2054 (1994) 32–42.
[14] H.R. Wilson, J.D. Cowan, Excitatory and Inhibitory Interactions in Localized

Populations of Model Neurons, Biophys. J. 12 (1972) 1–24.
[15] M.V. Tsodyks, W.E. Skaggs, T.J. Sejnowski, B.L. McNaughton, Paradoxical effects of external modulation of inhibitory interneurons, J Neurosci. 17 (1997) 4382–4388.
[16] R.A.E. Edden, N.A.J. Puts, A.D. Harris, P.B. Barker, C.J. Evans, Gannet: A batch-processing tool for the quantitative analysis of gamma-aminobutyric acid-edited MR spectroscopy spectra, J. Magn. Reson. Imaging 40 (2014) 1445–1452.
[17] Y. Zhang, M. Brady, S. Smith, Segmentation of brain MR images through a hidden Markov random field model and the Expectation-Maximization algorithm, IEEE Trans. Med. Imaging 20 (2001) 45–57.
[18] J.H. Yoon, R.J. Maddock, A. Rojem, M.A. Silver, M.J. Mizenberg, J.D. Ragland, C.S. Carter, GABA concentration is reduced in visual cortex in schizophrenia and correlates with orientation-specific surround suppression, J. Neurosci. 30 (2010) 3777–3781.
[19] G.E. Legge, J.M. Foley, Contrast masking in human vision, J. Opt. Soc. Am. 70 (1980) 1458–1471.
[20] D.G. Pelli, Uncertainty explains many aspects of visual contrast detection and discrimination, J. Opt. Soc. Am. A 2 (1985) 1508–1531.
[21] S. Treue, J.C.M. Trujillo, Feature-based attention influences motion processing gain in macaque visual cortex, Nature 399 (1999) 575–579.
[22] J.H. Reynolds, D.J. Heeger, The normalization model of attention, Neuron 61 (2009) 168–185.